

# Optics & Photonics in Sweden 2019 (OPS) 16-17 October 2019 Poster Abstracts

Kista, Stockholm at Electrum

**PhotonicSweden**  
*The Swedish Technology Platform in Optics and Photonics*



**Effective Structural Chirality of Beetle Cuticle Determined from Transmission Mueller Matrices Using the Tellegen Constitutive Relations**

*Hans Arwin, Linköping University*

**Line Confocal Imaging Sensors for Industrial Inspection**

*Murat Deveci, FocalSpec Ltd.*

**Backward lasing for range-resolved detection of atomic species**

*Pengji Ding, Lund University*

**Low-loss MEMS phase shifter for large scale reconfigurable silicon photonics**

*Pierre Edinger, Royal Institute of Technology (KTH)*

**Diamond gratings for dielectric laser acceleration**

*Pontus Forsberg, Uppsala University*

**Towards more efficient carbon dioxide and carbon monoxide concentration monitoring in cement factories using fibre-optic based gas monitoring systems**

*Kenny Hey Towa, RISE Fiber Optics*

**Toward XFEL Chip**

*Yen-Chieh Huang, National Tsing Hua University, Taiwan*

**Assessment of Fabrication Techniques for Large Aperture Quasi-Phase-Matched Device in RKTp**

*Cherry Lee, Royal Institute of Technology (KTH)*

**Simple semiconductor optical amplifier based tunable fiber laser architectures – innovative usage of chirped fiber Bragg gratings**

*Robert Lindberg, Royal Institute of Technology (KTH)*

**Fabrication of Widely Tunable Fiber Bragg Grating Filter Using Fused Deposition Modeling 3D Printing**

*Chunxin Liu, Royal Institute of Technology (KTH)*

**Subwavelength Adiabatic Multimode Y-junctions**

*Longhui Lu, KTH/Huazhong University of Science and Technology*

**Laser-based additive manufacturing of transparent fused silica glass**

*Pawel Maniewski, Royal Institute of Technology (KTH)*

**THz time-domain reflection spectroscopy of KTiOPO<sub>4</sub>**

*Kjell Martin Mølster, Royal Institute of Technology (KTH)*

**Postprocessing of semiconductor-core fibers -low loss waveguides and compositional microstructures**

*Korbinian Muehlberger, Royal Institute of Technology (KTH)*

**Recent progress in RKTp waveguides**

*Patrick Mutter, Royal Institute of Technology (KTH)*

**High-voltage fiber sensor based on fiber Bragg grating in poled fiber**

*Joao Pereira, RISE*

**Discrete and silicon-integrated InP-based photonic-crystal surface-emitting lasers**

*Carl Reuterskiöld Hedlund, Royal Institute of Technology (KTH)*

**Central and Peripheral Image Quality of the Human Eye**

*Dmitry Romashchenko, Royal Institute of Technology (KTH)*

**Simultaneous temporally and spectrally resolved Raman coherences with single-shot fs/ns rotational CARS**

*Maria Ruchkina, Lund University*

**Tunable flat magnetic lens**

*Georgii Shamuilov, Uppsala University*

**Performance Simulation and Function Analysis in Photoacoustic Tomography**

*Jiaqi Shi, Linköping University*

**Heteroepitaxy of Orientation-patterned GaP on GaAs Templates for Frequency Conversion Applications**

*Axel Strömberg, Royal Institute of Technology (KTH)*

**Micro- and Nanostructured TiO<sub>2</sub> Nanoparticles-Based Optical Coatings for LED and Solar Cell Applications**

*Dennis Visser, Royal Institute of Technology (KTH)*

**Intra-Cavity Up-Conversion Photon Counting Mid-Infrared Range Determination**

*Max Widarsson, Royal Institute of Technology (KTH)*

**Mueller Matrix Spectroscopic Tomography of Inhomogeneous Anisotropic Media**

*Qulei Xu, Linköping University*





# Effective Structural Chirality of Beetle Cuticle Determined from Transmission Mueller Matrices Using the Tellegen Constitutive Relations

• Hans Arwin<sup>1</sup>, Roger Magnusson<sup>1</sup>, Kenneth Järrendahl<sup>1</sup>, Stefan Schoeche<sup>2</sup>

1. Materials Optics, Department of Physics, Chemistry and Biology, Linköping University, SE-58183, Linköping, Sweden

2. J.A. Woollam Co., Inc., 645 M Street, Suite 102, Lincoln, NE 68508 USA

Several beetle species in the Scarabaeoidea superfamily reflect left-handed polarized light due to a circular Bragg structure in their cuticle whereas the right-handed polarized light is transmitted [1]. The objective here is to evaluate cuticle chiral properties in an effective medium approach using transmission Mueller matrices and compare with results obtained by electromagnetic modeling. The full constitutive relations are used which in the Tellegen representation are

$$\begin{aligned}\mathbf{D} &= \varepsilon_0 \boldsymbol{\varepsilon} \mathbf{E} + c_0^{-1} \boldsymbol{\xi} \mathbf{H} \\ \mathbf{B} &= c_0^{-1} \boldsymbol{\zeta} \mathbf{E} + \mu_0 \boldsymbol{\mu} \mathbf{H}\end{aligned}$$

where  $\varepsilon_0$  and  $\mu_0$  are the vacuum permittivity and permeability, respectively, and  $c_0$  the speed of light. Materials properties are given by the permittivity tensor  $\boldsymbol{\varepsilon}$ , the permeability tensor  $\boldsymbol{\mu}$  and the magnetoelectric tensors  $\boldsymbol{\xi} = \boldsymbol{\chi} + i\boldsymbol{\kappa}$  and  $\boldsymbol{\zeta} = -\boldsymbol{\xi}^T$ , where  $\boldsymbol{\chi}$  is the nonreciprocity tensor ( $\boldsymbol{\chi} = 0$  here) and  $\boldsymbol{\kappa}$  the chirality tensor. Transmission Mueller matrices are measured in the spectral range 350-1690 nm at normal incidence on the elytron from a *Cetonia aurata* beetle as shown in Fig. 1. Optical activity is observed in the antidiagonal with a resonance around  $\lambda=560$  nm.

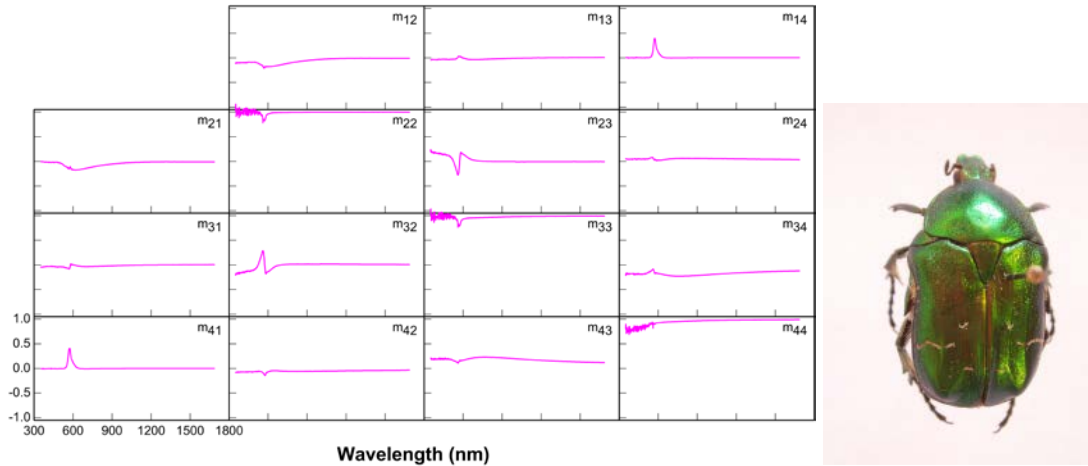


**Fig. 1** Normal incidence transmission Mueller matrix of an elytron from *Cetonia aurata*.

Non-linear regression analysis of the measured Mueller matrix using dispersion models for  $\boldsymbol{\kappa}$  and  $\boldsymbol{\varepsilon}$  provides a model spectrum of  $\kappa = \kappa_r + i\kappa_i$ . A differential decomposition of the Mueller matrix provides circular dichroism (CD) and circular birefringence (CB) spectra of the sample [2]. By estimating the sample thickness  $d$  and using the relation

$$\kappa = \kappa_r + i\kappa_i = -\frac{\lambda}{4\pi d} (CB + iCD)$$

agreements between the modeled and decomposed chirality are found.

[1] H. Arwin, T. Berlind, B. Johs and K. Järrendahl, *Cuticle Structure of Scarab Beetles Analyzed by Regression Analysis of Mueller-Matrix Ellipsometric Data*, Opt. Expr. **21**, 22645 (2013).

[2] H. Arwin, A. Mendoza-Galvan, R. Magnusson, A. Andersson, J. Landin, K. Järrendahl, E. Garcia-Caurel and R. Ossikovski, *Structural Circular Birefringence and Dichroism Quantified by Differential Decomposition of Spectroscopic Transmission Mueller Matrices from Cetonia Aurata*, Opt. Lett. **41**, 3293 (2016).

# Line Confocal Imaging Sensors for Industrial Inspection

Heimo Keränen, Murat Deveci\*

FocalSpec Ltd., Elektrononiikkatie 13, FI-90590 Oulu, Finland

---

## Abstract

Line Confocal Imaging (LCI) is an optical technology for high speed 2D and 3D topography and tomography measurements.

Line Confocal Imaging sensors measure millions of accurate 3D points per second, also from moving surfaces. The LCI sensors provide sub-micron resolution and can be used for all kind of surface types, including glossy, curved and transparent materials that have been challenging for industry standard laser sensors. Simultaneously with the 3D data, the LCI sensors produce also high dynamic range pixel synchronised intensity images of the surface which can be used to 2D defect detection and pattern recognition.

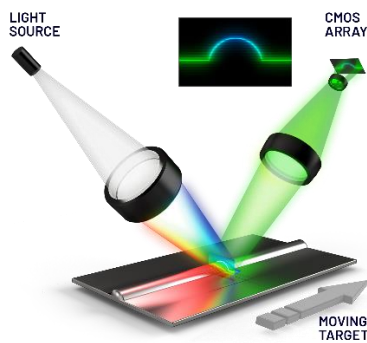


Figure 1 Basic working principle of LCI



Figure 2 LCI 1620 Sensor

The applications of LCI sensors include roughness measurement of transparent surfaces, defect detection in multilayer transparent materials, high speed dimensional control of 3D curved glasses, various surface and sub-surface analysis of flexible, hybrid, and organic electronics. The LCI sensors can be integrated to factory automation using Ethernet interface.

In this poster, the LCI will be explained in detail and several industrial applications will be given as examples.

**Keywords:** optical 3D sensors; surface metrology; film tomography, high-speed in-line inspection; submicron

\* Corresponding author. Tel.: + 358 50 467 4592  
E-mail address: [murat.deveci@focalspec.com](mailto:murat.deveci@focalspec.com)

# Backward lasing for range-resolved detection of atomic species

*Pengji Ding, Maria Ruchkina, Marcus Aldén, and Joakim Bood*

*Div. of Combustion Physics, Dep. of Physics, Lund University, Box 118, 221 00 Lund, Sweden*

*joakim.bood@forbrf.lth.se*

There is a strong need for sensitive methods able to measure at remote locations, i.e. remote sensing techniques. Such techniques are important not only in research, for example in atmospheric science, plasma and combustion chemistry, but also in many industrial applications as well as for fire safety and national security. The present talk concerns development of optical remote sensing concepts based on backward lasing, i.e. a mirror-less remote laser with a constituent of the ambient gas as the active medium. Lasing is accomplished in both the forward and backward direction through deep-UV multi-photon pumping of atoms using femtosecond (fs) laser pulses, as shown in Fig. 1. The focus of the talk is on spatially-resolved detection of atomic hydrogen in flames, yielding 656-nm lasing in the backward direction upon 2-photon pumping with 205-nm fs laser pulses. Spatial resolution is achieved by temporally-resolved detection of the backward lasing using a streak camera. The method is demonstrated in CH<sub>4</sub>/O<sub>2</sub> flames; both in a setup consisting of two flames, with variable spacing between the flames, and in a single flame. Although, the results demonstrate that the backward lasing technique is capable of detecting occurrences of hydrogen atoms in flames, further investigations are needed in order to extract quantitative concentrations. As a first step towards a deeper understanding of the signal generation mechanism, the gain of the hydrogen lasing has been studied.

It is evident that backward lasing could potentially revolutionize the remote-sensing field, as it might allow for a dramatic improvement of the detection sensitivity compared to traditional light detection and ranging (LIDAR), which is based on the detection of the nearly isotropic scattering induced by a forward-propagating laser beam. In addition, the high directionality of the backward lasing signal also opens up for measurements inside devices providing only one optical port. Besides detection of atoms and molecules in flames, the method also has potential for remote detection of atmospheric pollutants, gas leakage from pipelines, and the presence of explosives and hazardous materials.

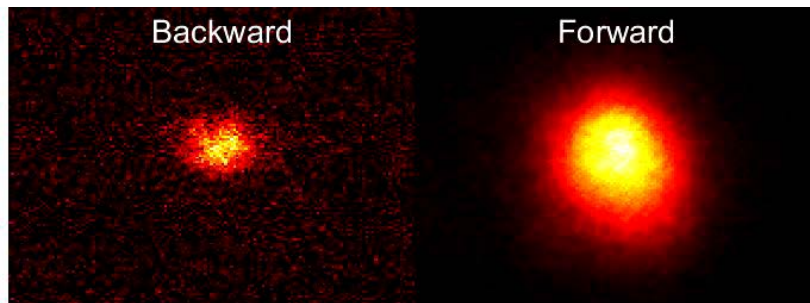


**Fig. 1** Backward and forward lasing at 656 nm from hydrogen atoms in a flame induced by femtosecond 2-photon pumping at 205 nm.

## Low-loss MEMS phase shifter for large scale reconfigurable silicon photonics

Photonic integrated circuits have shown the potential to become the next-generation multipurpose computing platform [1]. To keep up with the increasing demand for raw computational power and functionalities, large reconfigurable circuits are required. Current reconfigurable networks rely heavily on phase shifters as main active tuning elements (*Fig. 1*), and the traditional thermal actuation employed cannot keep up with the need for low-power consumption in large-scale circuits.

Photonic MEMS devices offer the ultra-low power actuation required for further upscaling, but previously reported phase shifters either show significant optical losses, or low tuning range. Longitudinal displacement of couplers enables large phase shifts for small displacements, but the full power coupling condition for low optical losses depends heavily on fabrication, due to the gap change upon release [2]. Direct electrostatic gap tuning of slot waveguides demonstrated phase shifts with very low footprint, but such slot waveguides are expected to be lossy [3].

We experimentally demonstrate a silicon MEMS phase shifter achieving more than  $\pi$  phase shift with sub-dB insertion loss (IL). The phase is tuned by reducing the gap between a suspended waveguide and a silicon beam, via comb-drive actuation (*Fig. 2*). The phase shift and Insertion Loss IL are extracted using a tunable laser and a Mach-Zehnder interferometer (*Fig. 3, Fig.4*). Our device reaches  $1.2\pi$  phase shift at only 20 V, with only 0.3 dB Insertion Loss. Finally, the device has a small footprint of  $50 \times 70 \mu\text{m}^2$  and its power consumption is 5 orders of magnitude lower than that of traditional thermal phase shifters. Our new phase-shifter is a fundamental piece of the next-generation large scale reconfigurable photonic circuits which find applications in interconnects for datacenters, A.I, or quantum computing.

### References

- [1] Pérez, Daniel, et al. "Multipurpose silicon photonics signal processor core." *Nature communications* 8.1 (2017): 636.
- [2] Ikeda, Taro, et al. "Phase-shifter using submicron silicon waveguide couplers with ultra-small electro-mechanical actuator." *Optics express* 18.7 (2010): 7031-7037.
- [3] – Van Acoleyen, Karel, et al. "Ultracompact phase modulator based on a cascade of NEMS-operated slot waveguides fabricated in silicon-on-insulator." *IEEE Photonics Journal* 4.3 (2012): 779-788.

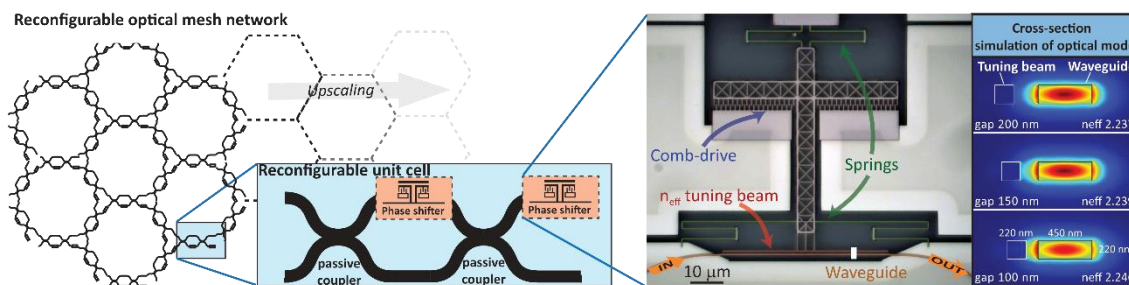


Figure 1. Large-scale photonic circuits rely on phase shifters for reconfiguration and to compensate for fabrication losses. The growing market of reconfigurable photonics circuits for applications in A.I or quantum computing requires an upscaling only possible with low-loss phase shifters.

Figure 2. Top view optical microscope image of our phase shifter. In-plane comb-drives actuators reduce the distance between a free silicon beam and a fixed waveguide. As a result, the effective index is tuned, which leads to a phase shift as light propagates through the interaction region.

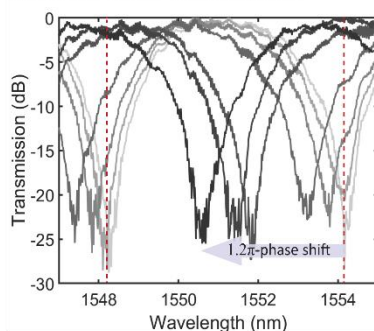


Figure 3. Measured transmission spectra for different actuation voltages. The device is inserted into one arm of a Mach Zehnder interferometer in order to measure the phase shift. A maximum phase shift of  $1.2\pi$  was obtained at 1550 nm.

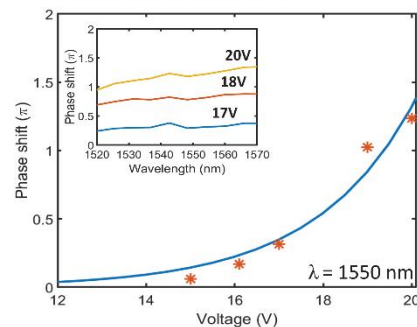


Figure 4. Measured data at 1550 nm with exponential fit. Inset: phase shift obtained with respect to wavelength. The device achieved a  $\pi$ -phase shift over 50 nm bandwidth.

# Diamond gratings for dielectric laser acceleration

Pontus Forsberg, Mathias Hamberg and Mikael Karlsson  
Uppsala University

The electric field strength in the focal spot of a femtosecond laser can be on the order of several GV/m. In dielectric laser acceleration (DLA) this strong electric field is harnessed to accelerate charged particles. A nano-structured dielectric surface is used to control the near field so that a particle, travelling close over the surface and in phase with a surface wave, will experience nearly continuous acceleration [1]. A limiting factor in DLA is that the laser intensity must not exceed the damage threshold of the dielectric material. The first demonstrations of DLA used fused silica gratings [1,2]. Peralta et al. [2] reported that at the high end of the energies they used, a peak electric field of  $\sim 3.5$  GV/m, they saw effects that they interpreted as structural damage. More recently, other grating geometries have been demonstrated in silicon. There are many well established fabrication processes for silicon, but it has a lower damage threshold than fused silica with a peak field around 1.4 GV/m [3].

In order to increase the peak electric field for accelerating particles, we are turning to materials that are likely to show improved resistance to laser damage. Diamond is a promising alternative, as it is well known as an extremely hard and chemically stable material. Initial tests by collaborators at Friedrich-Alexander Universität (FAU) in Erlangen have already showed that unstructured polycrystalline diamond samples were not damaged by pulses with a 4 GV/m peak field. Our first diamond DLA grating (fig. 1) has been fabricated in polycrystalline diamond using a process based on e-beam lithography, solvent assisted molding, and plasma etching. Laser ablation was then used to produce a raised structure with the grating on top. The diamond grating is currently awaiting testing at FAU. Future work includes making similar tests with single crystal diamond and sapphire, and potentially attempting a more advanced structure in either material.

- (1) John Breuer, Peter Hommelhoff, "Laser-Based Acceleration of Nonrelativistic Electrons at a Dielectric Structure", *Physical Review Letters* **111**, 134803, 2013.
- (2) E. A. Peralta et al., "Demonstration of electron acceleration in a laser-driven dielectric microstructure", *Nature* **503**, 92-94, 2013.
- (3) P. Yousefi et al., "Dielectric laser electron acceleration in a dual pillar grating with a distributed Bragg reflector", *Optics Letters* **44**(6), 1520-1523, 2019.

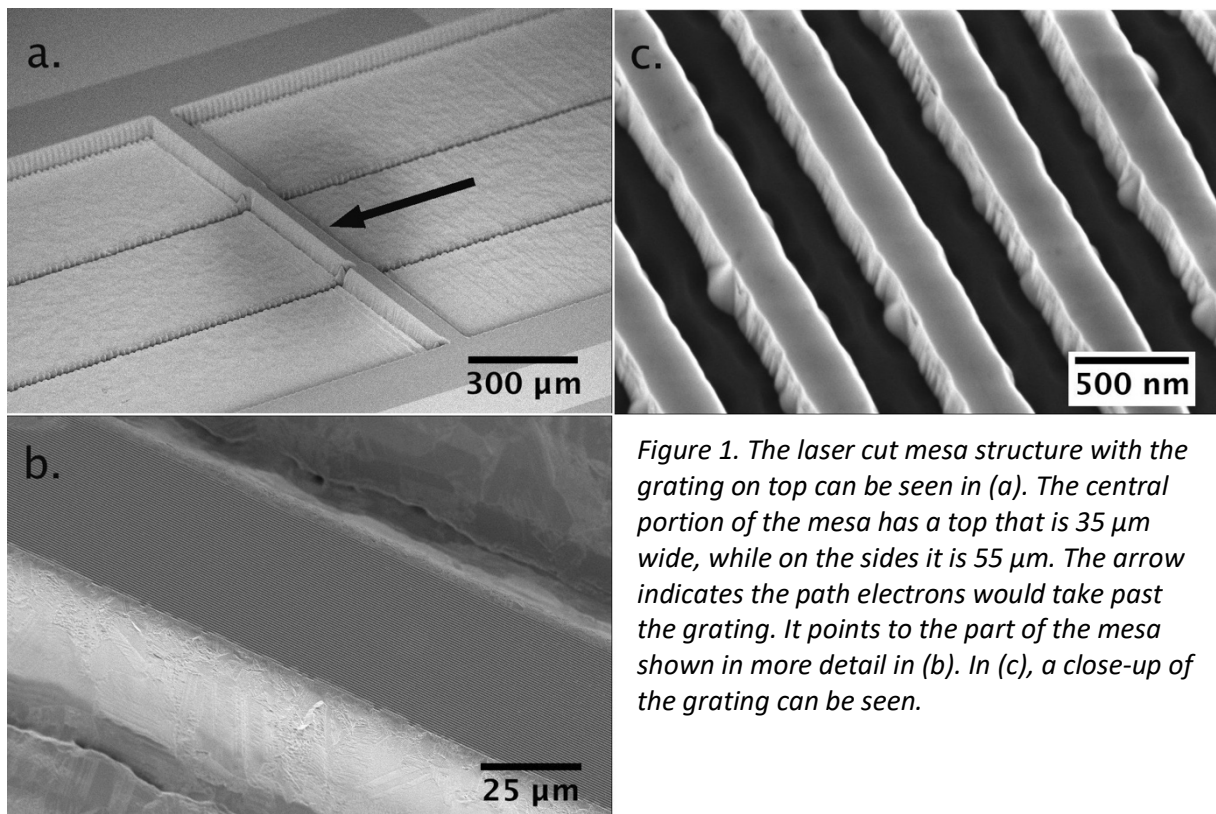


Figure 1. The laser cut mesa structure with the grating on top can be seen in (a). The central portion of the mesa has a top that is 35 μm wide, while on the sides it is 55 μm. The arrow indicates the path electrons would take past the grating. It points to the part of the mesa shown in more detail in (b). In (c), a close-up of the grating can be seen.

# Towards more efficient carbon dioxide and carbon monoxide concentration monitoring in cement factories using fibre-optic based gas monitoring systems

Kenny Hey Tow<sup>a,\*</sup>, Frans Forsberg<sup>a</sup> and Walter Margulis<sup>a</sup>

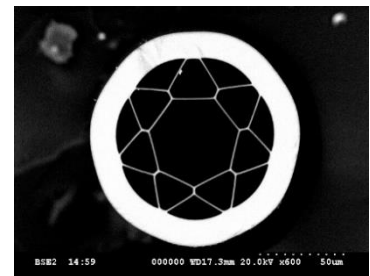
<sup>a</sup> RISE Acreo, Department of Fiber Optics, Electrum 236, 164 40, Kista, Sweden.

\* kenny.heytow@ri.se

## ABSTRACT

According to the Climate Act of June 2017, Sweden must achieve carbon-neutrality by 2045. Hence, regulations from the Swedish government to encourage the decarbonisation of emission-intensive activities will become increasingly important over the coming years. In particular, the cement industry is facing pressure to find technological solutions in reducing the large amount of greenhouse gas emissions since cement production is the source of around 8% of the world's CO<sub>2</sub> emissions, which is more than aviation fuel (2.5%) and not far behind the global agriculture business (12%). Vattenfall and Cementa AB are proceeding with ambitions to reduce the national CO<sub>2</sub> emissions by five percent by 2030 while the Research Institutes of Sweden (RISE) is active on a national strategy for a climate-neutral cement and concrete industry.

RISE Fibre Optic Department has been working towards offering more efficient fibre-optic based solutions for real-time CO and CO<sub>2</sub> gas monitoring during the combustion process. In this communication, an all-fibre gas monitoring system based on an anti-resonant hollow-core fibre is proposed. This special silica fibre (cross-section image on the right), designed and fabricated by RISE for gas sensing application has core and outer diameters of 50 and 125 µm respectively, and is single mode and transmits light from 1350 to beyond 1680 nm making it ideal for gas monitoring of low concentration of common pollutant gas such as CO, CO<sub>2</sub>, NO<sub>x</sub>, CH<sub>4</sub>, C<sub>2</sub>H<sub>2</sub>, etc. using wavelength modulation spectroscopy.



The performance of our optical fibre-based gas sensor was evaluated in the harsh environment (high temperature, dusty, corrosive, etc.) of a cement factory, Cementa (Slite). The concentration of CO<sub>2</sub> and CO in the flue gas, derived from raw material combustion, were simultaneously monitored during several hours and RISE's fibre-based sensor measurements showed good agreement with those given by an in-house commercial system used by Cementa.

## ACKNOWLEDGEMENTS

The authors would like to acknowledge Cementa AB (Sweden) and Vinnova, Sweden's innovation agency, for their support.

## Toward XFEL Chip

Yen-Chieh Huang

Institute of Photonics Technologies/Department of Electrical Engineering, National Tsing Hua University,  
Hsinchu 30013, Taiwan  
*ychuang@ee.nthu.edu.tw*

**Abstract:** The concept of chip-scale dielectric laser accelerator and laser undulator opens up the opportunity of an XFEL chip. Nano-electron bunches from the dielectric laser accelerator also enables chirped superradiance in the EUV spectrum, which can be further compressed to generate an isolated few-cycle EUV pulse. I will present a range of design parameters for an envisioned XFEL chip operating in the EUV and x-ray spectrum.

A dielectric laser accelerator (DLA) accelerates charged particles by using a phase synchronized laser field in an optical dielectric structure. Owing to the high damage threshold of a dielectric, a DLA is expected to provide stable particle acceleration with a gradient approaching 1 GeV/m. To be compact, a future free-electron laser (FEL) driven by a DLA would prefer a micro-undulator with a short undulator period and a high undulator field. One example is the proposed laser-pumped dielectric undulator in [1], which is fully compatible with the structure material and driver source of a DLA. A short undulator period means a low energy beam from an accelerator for a given radiation wavelength. When the radiation photon energy is not small compared with the electron kinetic energy, quantum recoil could knock the electron out of the FEL gain bandwidth. In such a quantum regime, one electron only emits one photon [2], resulting in poor radiation efficiency. On the other hand, a DLA, scaled by a laser wavelength, is unique in generating nano-meter electron bunches. Since the electron bunch length is already on the order of an x-ray wavelength, a DLA beam is well suited for generating intense coherent x-ray radiation or building up x-ray FEL (XFEL) radiation from a short undulator [3].

My study shows that, to saturate a hard x-ray FEL (wavelength  $< 0.1$  nm) in a 5~ 10 cm long dielectric laser undulator, it is desirable to have a beam energy  $> 300$  MeV, an undulator period of  $\sim 100$  microns, and a beam current of 10-20 kA. For soft x-ray FEL, one can avoid the disadvantageous quantum regime as long as the beam energy is larger than a few tens of MeV. By using a 50-MeV, 5-kA DLA beam in a cm long, 20- $\mu$ m-period laser undulator (gain length = 1 mm), a soft x-ray FEL can operate in the classic regime with an estimated peak output power of 22.5 MW at 1 nm wavelength. The average x-ray power from the soft XFEL can be in the mW range with a MHz electron pulse rate from the DLA. Therefore, a dielectric laser undulator driven by a DLA could be promising to realize a hand-held XFEL in the future. In my presentation, I will show a range of design parameters to avoid the disadvantageous quantum regime and yet take advantage of the short-bunch radiation for an ultra-compact XFEL driven by a low-energy DLA.

### References

- [1] T. Plettner, R. L. Byer, "Proposed dielectric-based microstructure laser-driven undulator," *Phys. Rev. ST Accel. Beams* **11**, 030704 (2008).
- [2] J. Gea-Banacloche, G. T. Moor, R. R. Schlicher, M. O. Scully, and H. Walther, "Soft x-ray free-electron laser with a laser undulator," *IEEE J. Quantum Electronics* **QE-23**, 1558-1570 (1987).
- [3] Y. C. Huang, R. L. Byer, "Ultracompact, high-gain, high-power free-electron lasers driven by future laser driven particle accelerators," *Proceedings of the Eighteenth International Free Electron Laser Conference*, G. Dattoli, A. Renieri (Eds.), Elsevier Science B.V., North-Holland, Amsterdam, II. 37 (1997).

# Assessment of Fabrication Techniques for Large Aperture Quasi-Phase-Matched Device in RKTP

Cherrie Lee\*, Andrius Zukauskas and Carlota Canalias

*Department of Applied Physics, KTH Royal Institute of Technology, Roslagstullsbacken 21, 10691 Stockholm, Sweden.*

\*csjlee@kth.se

## Abstract

For application in high energy optical parametric oscillators (OPO) and amplifiers (OPA), large aperture quasi-phase matching (QPM) devices are desirable as this allow pumping with larger beams and thus, larger pulse energy can be obtained. In most of the cases, the required period of these applications is in the range of 30-40  $\mu\text{m}$ . Recently, large-aperture (5 mm) Rb-doped  $\text{KTiOPO}_4$  (RKTP) has demonstrated excellent performance in a OPO configuration, generating 60 mJ of output energy [1].

For applications like quantum ghost imaging, which requires spontaneous parametric down conversion (SPDC) with wavelength down to 400 nm, large aperture QPM devices are also desirable. This sets a demand for large-aspect ratio domain structure with a periodicity down to 3  $\mu\text{m}$ .

Here we present the first results on fabrication of a 3 mm-thick periodically poled RKTP crystal with poling periodicity of 3.43  $\mu\text{m}$ . We show that conventional periodic poling techniques are not suitable to obtain a homogenous domain structure over the whole crystal aperture. Instead, fabrication of a coercive field grating [2], followed by periodic poling using planar electrodes is a much promising approach (see Figure 1).

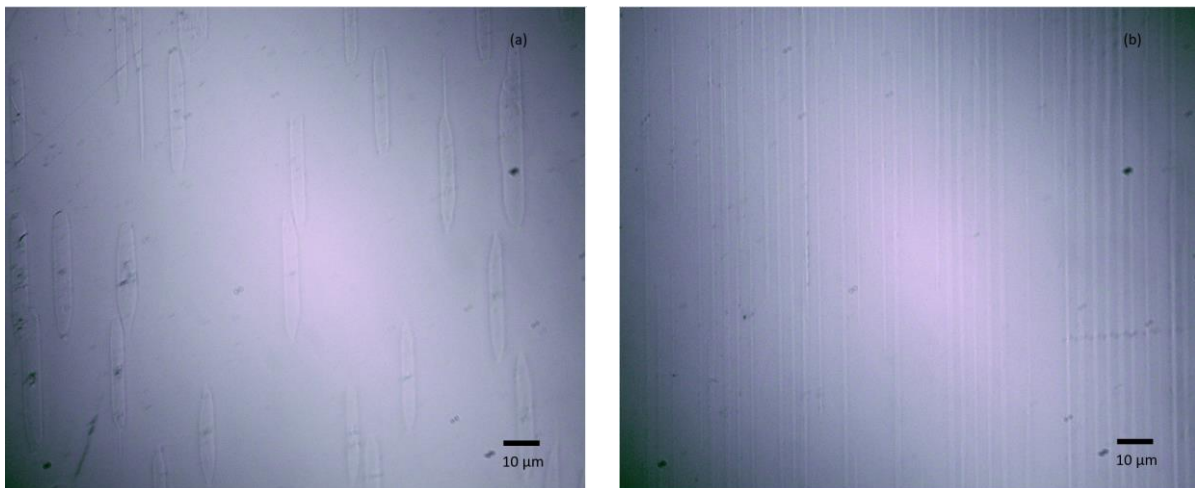


Figure 1 shows the etched domain structure on the RKTP crystal  $c^+$  face with a domain period of 3.43  $\mu\text{m}$ , obtained using (a) conventional poling technique (b) coercive field grating.

## References

- [1] Zukauskas, Andrius, et al. "5 mm thick periodically poled Rb-doped KTP for high energy optical parametric frequency conversion." *Optical Materials Express* 1.2 (2011): 201-206.
- [2] Liljestrand, Charlotte, Fredrik Laurell, and Carlota Canalias. "Periodic poling of Rb-doped  $\text{KTiOPO}_4$  by coercive field engineering." *Optics express* 24.13 (2016): 14682-14689.

# Simple semiconductor optical amplifier based tunable fiber laser architectures – innovative usage of chirped fiber Bragg gratings

R. Lindberg<sup>1\*</sup>, F. Laurell<sup>1</sup>, K. Fröjd<sup>2</sup> and W. Margulis<sup>1,3</sup>

<sup>1</sup> Department of Applied Physics, Royal Institute of Technology, 106 91 Stockholm, Sweden

<sup>2</sup> Proximion AB, Skalholtsgatan 10, SE 164 40 Kista, Sweden

<sup>3</sup> Department of Fiber Optics, RISE Acreo, 164 40 Kista, Sweden

rl@laserphysics.kth.se\*

Electrically tunable fiber lasers [1-3] are interesting for applications ranging from spectroscopy to optical coherence tomography. Here we present two very simple laser cavities, schematically illustrated in Fig. 1 a) - b), consisting of standard fiber components such as a semiconductor optical amplifier (SOA), a chirped Fiber Bragg grating (CFBG) to enable tunable operation, an output coupler (OC) and a circulator (Circ.). Driving the SOA with pulse sequences with differing temporal separations; denoted by  $T_1$ ,  $T_2$  and  $T$ , enables targeting of different regions on the CFBG and results in a tuned operating wavelength. This is illustrated for the two cavity configurations in Fig. 1 c) - d). A comparison of the principle of operation, an elaboration on the difference in laser performance as well as key characteristics and areas of application will also be presented.

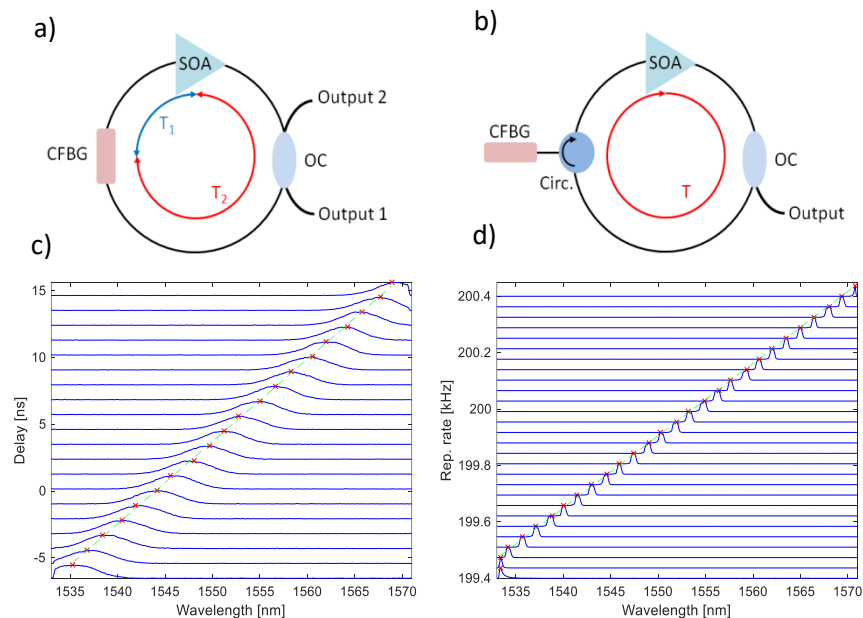


Fig. 1 Two different SOA-based laser designs are shown in a) and b). The corresponding tuning performance are given in the graphs directly below the two designs in c) and d).

[1] S. Li and K. T. Chan, IEEE Photon. Technol. Lett. 10(6), 799-801 (1998).

[2] X. Yang et al, Opt. Express 27, 14213-14220 (2019)

[3] T. Tiess et al, Opt. Lett. 42, 1125-1128 (2017)

# Fabrication of Widely Tunable Fiber Bragg Grating Filter Using Fused Deposition Modeling 3D Printing

CHUNXIN LIU,<sup>1</sup> XIONG YANG,<sup>1,3</sup> FREDRIK LAURELL,<sup>1</sup> AND MICHAEL FOKINE<sup>1</sup>

<sup>1</sup>*Department of Applied Physics, KTH Royal Institute of Technology, Stockholm 10691, Sweden.*

<sup>3</sup>*Centre for Optical and Electromagnetic Research (COER), Zhejiang University, 310058 Hangzhou, China*

**Abstract:** The use of 3D-printing for designing a simple wavelength tunable device based on fiber Bragg gratings is demonstrated. Using fused deposition modeling the fiber Bragg grating is embedded into a beam of polyethylene terephthalate glycol (PETG). Through bending, resulting in compression or tension of the optical fiber, the Bragg wavelength could be continuously tuned over a range of 60 nm, with maintained reflectivity and 3-dB linewidth.

# Subwavelength Adiabatic Multimode Y-junctions

Longhui Lu<sup>1,2</sup>, Max Yan<sup>2</sup>, and Mingming Zhang<sup>1</sup>

<sup>1</sup>School of Optical and Electronic Information, Huazhong University of Science and Technology, Wuhan, Hubei 430074, China

<sup>2</sup>Department of Applied Physics, KTH Royal Institute of Technology, Stockholm 16440, Sweden  
email: miya@kth.se, mmz@hust.edu.cn

**Keywords:** subwavelength, multimode, silicon photonics, Y-junction

## Abstract

Adiabatic multimode Y-junctions are extensively used in multimode silicon photonics devices due to their straightforward principle in achieving mode splitting and manipulation [1]. However, majority of the reported studies on multimode Y-junctions are limited to simulation work; experimentally, limited feature size achievable by lithography can greatly deteriorate the adiabatic branching property and result in large excess loss and crosstalk [2, 3]. For an ideal multimode Y-junction, there is a tapered slot between the two branch waveguides, and the slot width gradually increases from ideally zero to a certain gap width [Fig. 1(a)]. Instead of using a continuous tapering, we propose an effective tapered slot based on subwavelength chirped circular holes [Fig. 1(b)]. By optimizing the holes' radii and positions in the chirped subwavelength slot under our fabrication constraint, we can realize an effective width increasing from zero to a certain width adiabatically. We, for the first time to our knowledge, fabricated and characterized both subwavelength adiabatic symmetric and asymmetric four-mode Y-junctions respectively, and found low, mode-independent excess loss and crosstalk profiles. Such junctions are broadband, compact, CMOS-compatible, tolerant to fabrication error, and can be extended for operation with more modes.

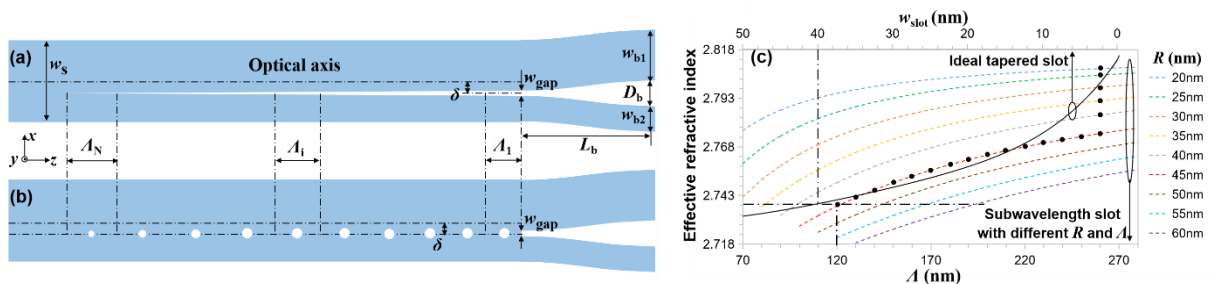


Fig. 1. Adiabatic multimode Y-junction based on (a) an ideal tapered slot, or (b) a circular-hole-based chirped subwavelength slot. (c) Effective refractive index evolution profiles of TE<sub>0</sub> mode in the ideal tapered slot waveguide and the chirped subwavelength slot waveguide of a symmetric four-mode Y-junction.

## References

- [1] J. D. Love, and N. Riesen, "Single-, few-, and multimode Y-junctions," *J. Lightw Technol.* **30**, 304-309 (2012).
- [2] C. Sun, Y. Yu, and X. Zhang, "Ultra-compact waveguide crossing for a mode-division multiplexing optical network," *Opt. Lett.* **42**, 4913-4916 (2017).
- [3] W. Chen, P. Wang, T. Yang, G. Wang, T. Dai, and Y. Zhang, "Silicon three-mode (de) multiplexer based on cascaded asymmetric Y-junctions," *Opt. Lett.* **41**, 2851-2854 (2016).
- [4] L. Lu, D. Liu, M. Yan, M. Zhang, "Subwavelength adiabatic multimode Y-junctions," *Opt. Lett.* **44**, 4729-4732 (2019).

# Laser-based additive manufacturing of transparent fused silica glass

Pawel Maniewski, Fredrik Laurell, Michael Fokine

Laser physics group, School of Engineering Science, KTH Royal Institute of Technology, Stockholm, Sweden

Corresponding author: [pawelma@kth.se](mailto:pawelma@kth.se)

## Abstract

Additive manufacturing of various types of materials and geometries ensures sustainability in the production of modern devices. Fused silica glass is a high demand material, while its production can be challenging and expensive due to its high melting temperature. Here we present research results in the development of additive manufacturing of transparent fused silica glass. A CO<sub>2</sub>-laser is used for laser sintering of fused silica, and for post-processing by laser beam scanning across the deposited layers. High powder efficiency, up to 30% by weight, has been demonstrated. In-line post-processing of deposited fused silica layers has shown to provide significantly increased surface quality and transparency of the glass as showed in Fig. 1.

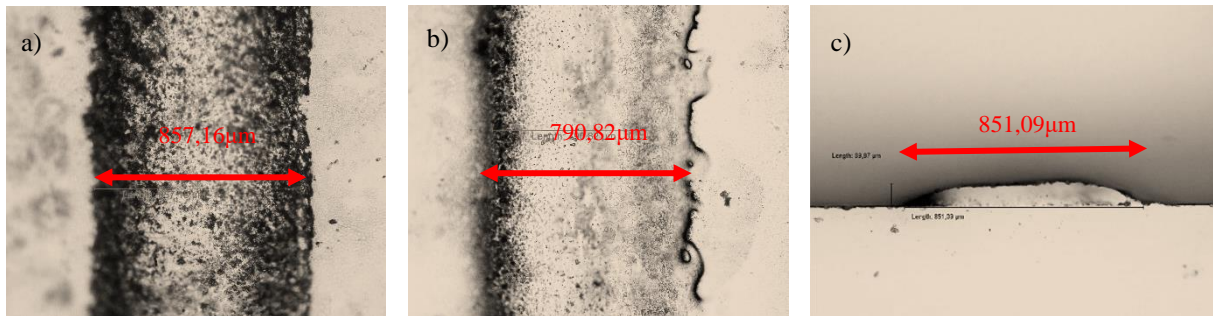


Fig. 1. Microscopic images of a) as deposited fused silica layer, b) partially (left side) post-processed fused silica layer, and c) polished cross section of layer shown in b).

# THz time-domain reflection spectroscopy of $\text{KTiOPO}_4$

Kjell Mølster<sup>1,2</sup>, Hugo Laurell<sup>3</sup>, Trygve Sörgård<sup>4</sup>, Carlota Canalias<sup>2</sup>, Valdas Pasiskevicius<sup>2</sup>  
Fredrik Laurell<sup>2</sup>, Ulf Österberg<sup>1,2</sup>

1. Department of Electronic Systems, Norwegian University of Natural Science and Technology, N-7491, Trondheim, Norway

2. Department of Applied Physics, Royal Institute of Technology, KTH, 10691 Stockholm, Sweden

3. Division of Atomic Physics at the Faculty of Engineering (LTH), Lund University, Lund, Sweden

4. Department of Physics, Norwegian University of Science and Technology, Trondheim NO-7491, Norway

There is an ongoing development of THz sources for high-field applications, especially with the view of potential for THz-driven particle accelerators. For such sources nonlinear materials with high optical damage threshold and low loss are required.  $\text{KTiOPO}_4$ , (KTP) is a well-established material for nonlinear optical applications in the visible and near-IR region thanks to its large transparency, high nonlinear coefficient and damage threshold. Its reasonably low absorption [1, 2] and strong coupling to phonon-polariton degree of freedom [1]. This shows promise for efficient IR to THz conversion process. Indeed, Wu *et al.* [2] recently demonstrated its superiority to  $\text{LiNbO}_3$  and  $\text{LiTaO}_3$  in a back to back experiment. In view of this, it is important to determine the spectrum of complex refractive index over larger spectral range and with higher accuracy than has been do so far. KTP is an orthorhombic crystal belonging to  $\text{mm}2$  point group with a rather complex vibrational mode structure containing 192 degrees of freedom. Earlier spectroscopic studies of KTP have either lacked the possibility of directly extracting the complex refractive index [3] or been limited by absorption of the transmitted signal due to the strong resonances of KTP, limiting the spectral extent to about 2.5 THz [4]. In this work we utilize reflection THz time-domain spectroscopy (TTDS) to determine the spectrum of the refractive index,  $n$ , and the absorption coefficient,  $\alpha$ , between 0.5 THz and up to 7 THz for two eigenpolarizations on the (001) plane.

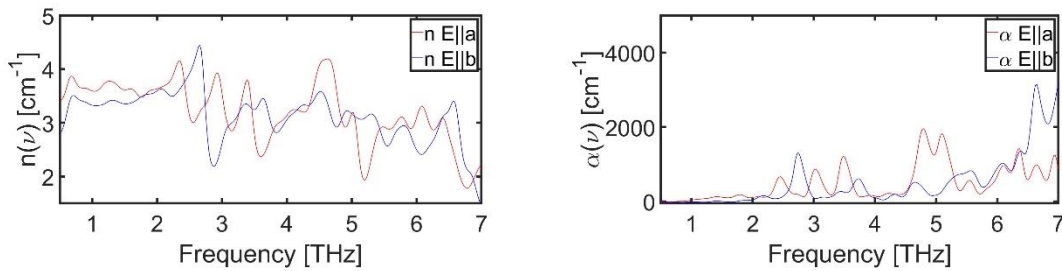


**Fig. 1** (LEFT) The measured refractive index along the crystallographic a-axis (RED) and b-axis (BLUE). (RIGHT) The measured absorption coefficient for a-axis (RED) and b-axis (BLUE).

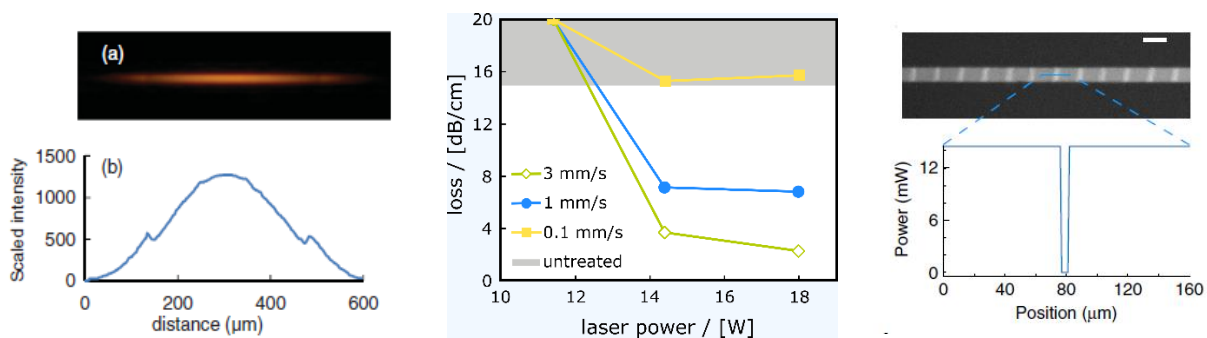
## References

- [1] H. Jang, G. Strömqvist, V. Pasiskevicius, C. Canalias, “Control of forward stimulated polariton scattering in periodically-poled KTP crystals,” *Opt. Express* 21 27277 (2013).
- [2] M.-H. Wu, Y.-C. Chiu, T.-D. Wang, G. Zhao, A. Zukauskas, F. Laurell, and Y.-C. Huang, “Terahertz parametric generation and amplification from potassium titanyl phosphate in comparison with lithium niobate and lithium tantalate”, *Opt Express*. **24**, 25964 (2016).
- [3] B. Wyncke, F. Brehat, J. Mangin, G. Marnier, M. F. Ravet, and M. Metzger, “Infrared reflectivity spectrum of  $\text{KTiOPO}_4$  single crystal,” *Phase Transitions* 9, 179–183 (1987).
- [4] V. D. Antsygin, A. B. Kaplun, A. A. Mamrashev, N. A. Nikolaev, and O. I. Potaturkin, “Terahertz optical properties of potassium titanyl phosphate crystals,” *Opt. Express* 22, 25436 (2014).

## Postprocessing of semiconductor-core fibers -low loss waveguides and compositional microstructures-

Korbinian Mühlberger, Taras Oriekhov, Fredrik Laurell, Ursula Gibson, Michael Fokine  
*Royal Institute of Technology, Applied Physics, Stockholm, 106 91, Sweden.*

Semiconductor-core fibers, integrating the optical and electronic properties of semiconductors within a long flexible optical fiber geometry, is an emerging research field with numerous potential applications in photonics and optoelectronics due to large nonlinear optical coefficients and an extended transparency window. Manufactured with a drawing tower, their as-drawn quality is not suitable for optical purposes since the semiconductors are neither mono-crystallized nor is the local composition of compound semiconductors controlled. Here it is shown, how these hinders can be overcome by suitable postprocessing with irradiation of a CO<sub>2</sub> laser beam. The fiber geometry offers the unique possibility to melt the core by heating the cladding, where the latter acts as a crucible. By controlling various parameters (temperature of the fiber core, size of the localized melt-zone and the velocity at which the melt-zone is shifted through the fiber), it is possible to drastically reduce optical transmission losses and inscribe microstructures for various optical applications.



### Acknowledgments:

The project activities are supported by Stiftelsen for Strategisk Forskning (SSF) grant RMAI5- 0135, and the Knut and Alice Wallenberg Foundation (KAW) grant 2016.0104.

### REFERENCE

- [1] N. Healy, M. Fokine, Y. Franz, T. Hawkins, M. Jones, J. Ballato, A. C. Peacock, U. J. Gibson, "CO<sub>2</sub> Laser-Induced Directional Recrystallization to Produce Single Crystal Silicon-Core Optical Fibers with Low Loss," *Advanced Optical Materials*, 4(7), 1004-1008 (2016).
- [2] D. A. Coucheron, M. Fokine, N. Patil, D. W. Breiby, O. T. Buset, N. Healy, A. C. Peacock, T. Hawkins, M. Jones, J. Ballato, U. J. Gibson, "Laser recrystallization and inscription of compositional microstructures in crystalline SiGe-core fibres," *Nature Communications*, 7, 13265 (2016).

## Recent progress in RKTp waveguides

Patrick Mutter\*, Cristine C. Kores, Hoda Kianirad, Fredrik Laurell and Carlota Canalias

Department of Applied Physics, Royal Institute of Technology, Roslagstullbacken 21, 10691, Stockholm, Sweden

\*pmutter@kth.se

Waveguides, as part of integrated photonics offer a high level of robustness, stability and compactness compared to traditional optical setups. Additionally, waveguides offer high confinement over long interaction lengths which provide means for highly efficient nonlinear interactions.

This work presents the recent progress in waveguide fabrication in quasi-phase matched bulk Rb-doped  $\text{KTiOPO}_4$  (RKTp). This material provides the possibility of fabricating stable waveguides at high powers, which is known to be a problem in ordinary flux grown KTP [1]. Furthermore, the reduced ionic conductivity of RKTp allows to pole these crystals with much shorter periods which enables to study novel nonlinear processes such as mirrorless parametric oscillators [2] in the waveguide format. Two different fabrication schemes have been investigated: Diced waveguides (see Figure 1) [3] and channel waveguides. Moreover, the key parameters in order to maintain high conversion efficiency in periodically poled waveguides have been identified. The waveguides in this work demonstrate efficient blue second harmonic generated light via type 0 phase matching. The waveguides reached a normalized conversion efficiency of  $158 \frac{\%}{\text{Wcm}^2}$ .

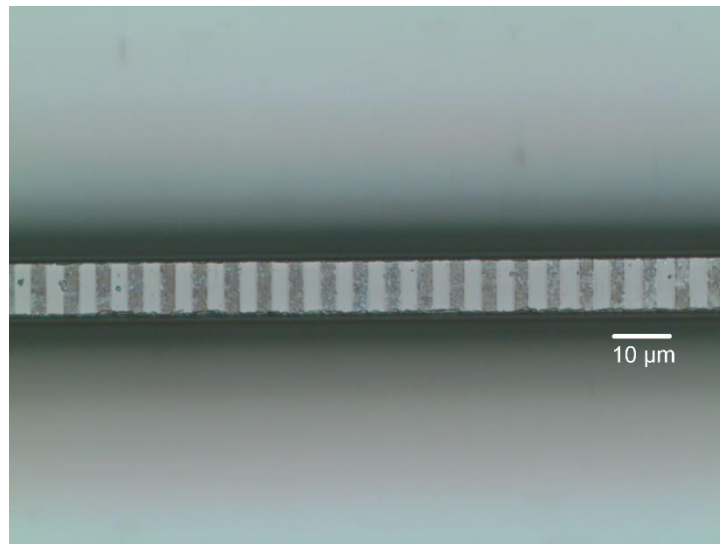


Figure 1: Top picture of ridge waveguide

- [1] F. Laurell, "Periodically poled materials for miniature light sources," *Opt. Mater. (Amst)*., vol. 11, no. 2–3, pp. 235–244, 1999.
- [2] C. Canalias and V. Pasiskevicius, "Mirrorless optical parametric oscillator," pp. 459–462, 2007.
- [3] C. C. Kores, P. Mutter, H. Kianirad, C. Canalias, and F. Laurell, " Quasi-phase matched second harmonic generation in periodically poled Rb-doped  $\text{KTiOPO}_4$  ridge waveguide ," *Opt. Express*, vol. 26, no. 25, p. 33142, 2018.

# High-voltage fiber sensor based on fiber Bragg grating in poled fiber

J. M. B. Pereira<sup>\*1,2</sup>, J. Hervás<sup>3</sup>, D. Barrera<sup>3,4</sup>, J. Madrigal<sup>3</sup>, S. Sales<sup>3</sup>, F. Laurell<sup>2</sup>, O. Tarasenko<sup>1</sup>, W. Margulis<sup>1,2</sup>

<sup>1</sup>Fiber Optics, RISE Acreo, Electrum 236, 16440, Kista, Sweden.

<sup>2</sup>Dep. of App. Phys., KTH, Roslagstullsbacken 21, 10691, Stockholm, Sweden.

<sup>3</sup>TEAM Research Institute, Universitat Politècnica de València, Valencia 46022, Spain.

<sup>4</sup>Dept. of Electronics, University of Alcalá, Alcalá de Henares, 28805, Spain.

Email: [joao.pereira@ri.se](mailto:joao.pereira@ri.se)

## Abstract

Fiber Bragg gratings (FBG's) inscribed in twin-hole fiber with internal electrodes are evaluated to measure high-voltage. The proposed interrogation system is simple to build and is an open-ended arrangement, suitable for remote sensing long distances. The setup can have many voltage sensors if different FBG's are used. The sensor described can be used in high-voltage transmission lines or power plants for remote sensing different points with one fiber end.

The fiber utilized shares the same optical characteristics of a standard telecom fiber; it is low-loss and easy to splice. The internal electrodes are one meter long and made of BiSn pumped in molten state inside the twin-hole fiber. To enhance the voltage sensitivity, the fiber was optically poled with a second-harmonic Nd:YAG Q-Switched and mode-locked laser, technique and special fiber described in [1]. Poling induces a linear electro-optic effect by recording an electric-field inside the material. The non-linearity induced to the fiber is 0.086 pm/V.

A lock-in amplifier can be used to detect a known frequency and increase device sensitivity. This is a work in progress, and new measurements to evaluate cut-off frequencies, input impedances, and dynamic range are being realized.

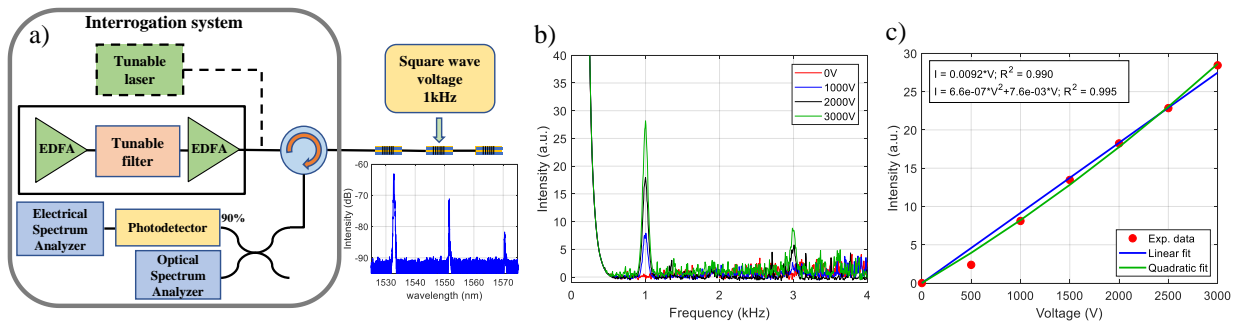


Figure 1 – a) Interrogation system. b) Spectral response for different voltages. c) Intensities of the electrical spectrum at 1 kHz.

## References

- [1] A. R. Camara, J. M. B. Pereira, O. Tarasenko, W. Margulis and I. C. S. Carvalho, "Optical creation and erasure of the linear electrooptical effect in silica fiber," *Optics Express*, vol. 23, pp. 18060-18069, 2015.

## Acknowledgments

The authors acknowledge financial support from the FINESSE project. FINESSE is funded by the European Union's Horizon 2020 research and innovation program under the Marie Skłodowska Curie grant agreement n° 722509. Partial funding from K. A. Wallenberg Foundation and the Swedish Science Council is gratefully acknowledged.

# Discrete and silicon-integrated InP-based photonic-crystal surface-emitting lasers

Carl Reuterskiöld Hedlund<sup>1,\*</sup>, Joao Martins De Pina<sup>1</sup>, Shih-Chia Liu<sup>2</sup>, Deyin Zhao<sup>2</sup>, Weidong Zhou<sup>2</sup>, and Mattias Hammar<sup>1</sup>

<sup>1</sup>Department of Electrical Engineering, Royal Institute of Technology, Electrum 229, 164 40 Kista, Sweden

<sup>2</sup>Department of Electrical Engineering, University of Texas at Arlington, TX 76019, USA

\*Corresponding author: CarlRH@KTH.se

Photonic-crystal surface-emitting lasers (PCSELS) have the potential for large-area singlemode emission by virtue of Bragg reflection from a two-dimensional standing-wave mode confined by a buried photonic crystal (PC) layer in close proximity to an activated gain region<sup>1</sup>. Here we report on the fabrication of 1.55- $\mu\text{m}$  PCSELS in two different configurations, either by direct integration on silicon, resulting in an ultra-shallow devices with potential applications in CMOS photonics<sup>2</sup>, or a bulk InP device designed for very-high power operation. In the former case, transfer printing is used to add an InP active membrane on a PC-structured silicon-on-insulator substrate, and a buried tunnel junction configuration is used for efficient and uniform current injection also for devices up to  $80\times 80\text{-}\mu\text{m}^2$  in area<sup>3</sup>. This device is schematically illustrated in Fig. 1 a). For the bulk InP PCSELS, a buried and periodic semiconductor/air PC structure is realized using an etching and metal-organic vapor-phase epitaxial regrowth process. Electron-beam lithography and an inductively coupled plasma etching process is used to define high-aspect ratio holes in the InP substrate and by careful tuning of the growth parameters it is possible to close these holes before they are filled with InP, thereby forming embedded voids in the crystal lattice as shown in Fig. 2 a). The final device, relying on front-side as well as backside processing and contacting is schematically illustrated in Fig. 2 b).

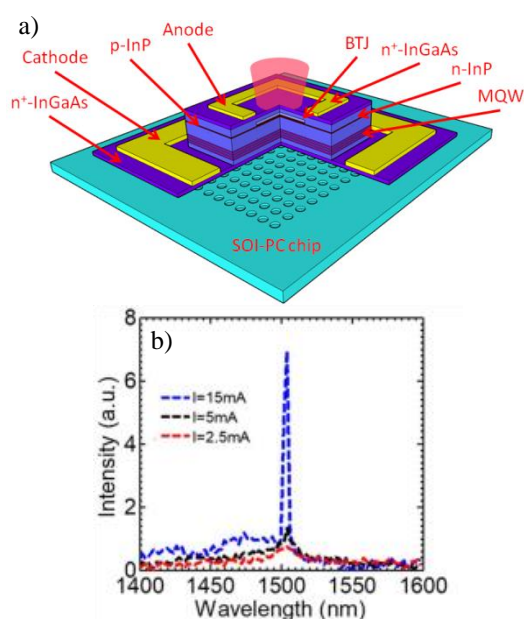


**Figure 1.** a) Schematic illustration of the InP membrane/silicon PC hybrid device. The thickness of the InP slab is only  $\sim 0.5\ \mu\text{m}$  as compared to  $\sim 10\ \mu\text{m}$  for a conventional VCSEL. b) Emission spectrum under electrical injection of an  $80\times 80\text{-}\mu\text{m}^2$  device.

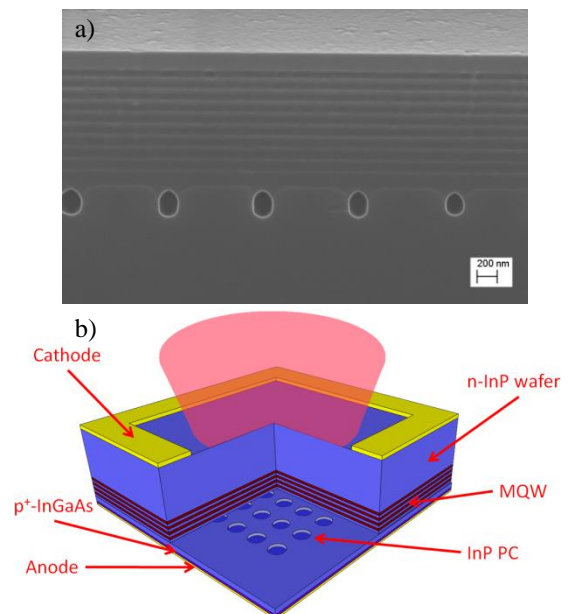


**Figure 2.** a) Scanning electron microscopy image of a cleaved PC lattice formed by etching and epitaxial regrowth. The contrast is due to stain-etching and differently doped regions. The layers above the PC demonstrates the planar growth evolution. b) Schematic illustration of the final device configuration.

<sup>1</sup> K. Hirose, Y. Liang, Y. Kurosaka, A. Watanabe, T. Sugiyama, and S. Noda, Nat. Photonics 8, 406 (2014)

<sup>2</sup> D. Zhao, S.-C. Liu, H. Yang, Z. Ma, C. Reuterskiöld Hedlund, M. Hammar, W. Zhou, Scientific Reports 6, 18860 (2016)

<sup>3</sup> C. Reuterskiöld Hedlund, SC Liu, D Zhao, W Zhou, M Hammar, Phys. Status Solidi A, 1900527 (2019)

## **“Central and Peripheral Image Quality of the Human Eye”**

Dmitry Romashchenko, MSc

Petros Papadogiannis, MSc

Peter Unsbo, PhD

Linda Lundström, PhD

*Department of Applied Physics, Royal Institute of Technology, Stockholm, Sweden*

### **Abstract**

Peripheral image quality influences several aspects of human vision. Apart from off-axis visual functions, the manipulation of peripheral optical errors is widely used in myopia (near-sightedness) control interventions. This, together with recent technological advancements enabling the measurement of peripheral errors, has inspired many studies concerning off-axis optical aberrations. However, direct comparison between these studies is often not straightforward. To enable between-study comparisons and to summarize the current state of knowledge, this review presents population data analyzed using a consistent approach from 16 studies on peripheral ocular optical quality (in total over 2,400 eyes). The presented data include refractive errors and higher order monochromatic aberrations expressed as Zernike coefficients (reported in a subset of the studies) over the horizontal visual field. Additionally, modulation transfer functions, describing the monochromatic image quality, are calculated using individual wavefront data from three studies. The analyzed data show that optical errors increase with increasing eccentricity as expected from theoretical modelling. Compared to emmetropes (subjects with no central refractive error), myopes (subjects with near-sightedness) tend to have more positive relative peripheral refraction over the horizontal visual field and worse image quality in the near-periphery of the nasal visual field. The data collated in this review are important for the design of ocular corrections and the development and assessment of optical eye models.

# Simultaneous temporally and spectrally resolved Raman coherences with single-shot fs/ns rotational CARS

*Ali Hosseinnia, Maria Ruchkina, Pengji Ding, Per-Erik Bengtsson, Joakim Bood*

*Div. of Combustion Physics, Dep. of Physics, Lund University, Box 118, 221 00 Lund, Sweden  
joakim.bood@forbrf.lth.se*

A novel technique for studies of the dynamics of molecular coherences has been developed. The concept is based on prompt excitation using broadband femtosecond laser pulses, whereupon a narrowband nanosecond laser pulse probes the fast dynamics of the coherences. Detection of the spectrally dispersed coherent signal using a streak camera allows simultaneous spectrally and temporally resolved studies of all excited coherences in a single-shot acquisition. Here we demonstrate the high capacity and versatility of this hybrid femtosecond/nanosecond coherent anti-Stokes Raman scattering (CARS) technique through some illustrative examples, all single-shot measurements, namely time-resolved studies of rotational Raman coherences in nitrogen and air, dynamics of Stark effect on rotational lines, and beating phenomena originating from close-lying rotational lines. Figure 1 shows spectrally and temporally resolved rotational CARS signal of nitrogen and argon recorded in a single shot at ambient conditions.

To the best of our knowledge, this is the only technique with the capacity to probe the full temporal and spectral evolution of molecular coherences on a single-shot basis. It is evident that the technique opens the door to a multitude of fundamental molecular studies as well as applications. One such area is plasma physics, where the fast and stochastic events require high temporal resolution and single-shot detection. Another area is in turbulent reactive flows, where methods for accurate gas-phase thermometry are lacking.

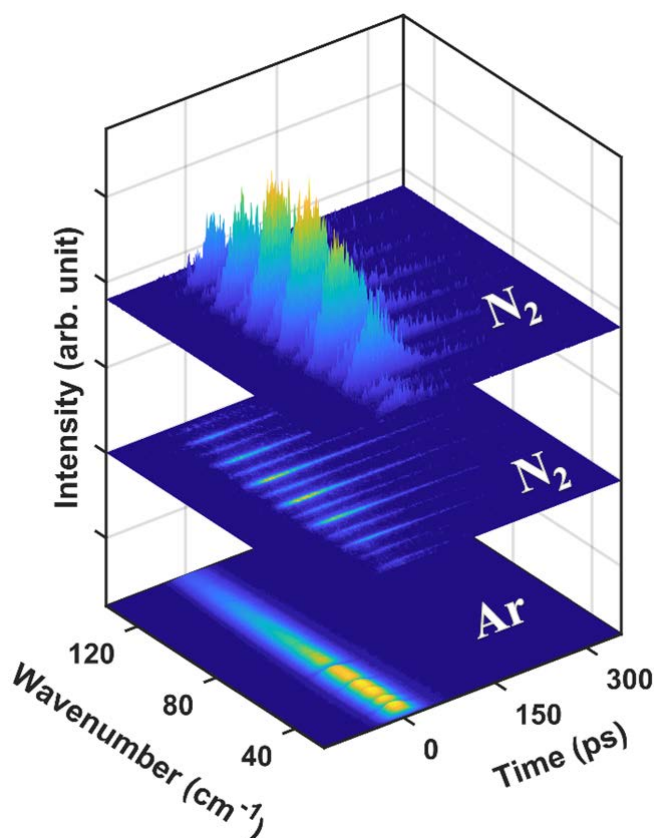


**Fig. 1** The upper two plots show a spectrally and temporally resolved rotational CARS signal of nitrogen recorded in a single shot at ambient conditions. The plot at the bottom shows signal from argon, averaged over 200 single shots. Being an atom, lacking rotational structure, this signal does not exhibit any rotational lines, but only non-resonant contribution. The spectral and temporal characteristics of this signal thus reflect the spectral and temporal instrument response, respectively. The sharp stripes visible in the argon signal are artefacts due to imperfections in the detection system.

# Tunable flat magnetic lens

Georgii Shamuilov<sup>1</sup>, Alexey Nikitin<sup>2,3,4</sup> and Vitaliy Goryashko<sup>1</sup>

- <sup>1</sup> FREIA Laboratory, Department of Physics and Astronomy, Uppsala University, Lägerhyddsvägen 1, Uppsala, 75120 Sweden; phone: +46(18)471-32-53;
- <sup>2</sup> Donostia International Physics Center (DIPC), Donostia-San Sebastian, 20018, Spain
- <sup>3</sup> IKERBASQUE, Basque Foundation for Science, Bilbao, 48013, Spain
- <sup>4</sup> CIC nanoGUNE, Donostia-San Sebastian, 20018, Spain

E-mail: [georgii.shamuilov@physics.uu.se](mailto:georgii.shamuilov@physics.uu.se)

**Abstract:** We present a concept of a tunable, sub-wavelength-thick electromagnetic lens. The lens is based on oscillating quasi-two-dimensional electron gas immersed into an axially symmetric magnetic field with non-uniform strength (a coil). For a general antisymmetric tensor of the dielectric permittivity, we extract the phase advance and demonstrate the focusing effect. Exploring the parameter space, we apply this procedure to the case of graphene for waves in the terahertz frequency range. In addition, we discuss other materials, conducting, such as silver, and dielectric, such as ferrites. As an extension, such a lens can be deposited on a surface of a conventional plano-convex lens to allow for fine tuning of the focal length of the latter.

**Keywords:** planar optics, phase advance, wavefront control, graphene, non-uniform fields

# Performance Simulation and Function Analysis in Photoacoustic Tomography

Jiaqi Shi<sup>a,b</sup>, Yingjie Yu<sup>a</sup>, Sergiy Valyukh<sup>b,\*</sup>

<sup>a</sup>*Department of Precision Mechanical Engineering, Shanghai University, Shanghai 200072, China*

<sup>b</sup>*Department of Physics, Chemistry and Biology, Linköping University, SE-581 83 Linköping, Sweden*

\*email: [sergiy.valyukh@liu.se](mailto:sergiy.valyukh@liu.se)

**Abstract:** Photoacoustic imaging is a new non-invasive and highly informative biological imaging method developed rapidly in recent years [1], which is based on the photoacoustic effect. A biological tissue under study is illuminated by laser pulses, energy of which is absorbed and converted into heat causing transient thermoelastic expansion. The thermoelastic expansion is investigated with ultrasonic emission spatial analysis of transmission of which enable us to obtain an image of the inner structure [2]. In order to clear understand the mechanisms in photoacoustic tomography, correctly interpret a measured information and obtain optimal conditions in an experiment, it is necessary to carry out simulation of the physical processes used. Our work is devoted to such a simulation. Light energy transmission through the tissues from the laser source is described by diffusion equation. The absorption of light and thermoelastic expansion can be modeled with bio-heat equation [3, 4]. The resulting stress caused by the heat and the strain change are included to the acoustic wave equation [5] that describes propagation of ultrasound. Numerical solutions of all these differential equations we obtain by using the finite element method implemented in commercial software COMSOL Multiphysics. Visualization of the temperature distribution caused by energy conversion and resulting pressure and strain are carried out by using a cylindrical finite element model. The optical and acoustic parameters are optimized by the simulation in the considered model. Scattering and absorption can be analyzed to provide more information on a photoacoustic system and can be included in tissue models as the next step of the simulation.

**Keywords:** Photoacoustic, Simulation, Parameter, Analysis, Image

## **References:**

- [1] M. Li, Y. Tang, J. Yao, *Photoacoustics*, 10, 65-73 (2018).
- [2] P. J. van den Berg, K. Daoudi, W. Steenbergen, *Photoacoustics*, 3(3), 89-99 (2015).
- [3] S. Jeon, J. Kim, D. Lee, J. W. Baik, C. Kim, *Photoacoustics*, 15, 100141 (2019).
- [4] Z. Wang, S. Ha, K. Kim, *Proc. SPIE 8223*, 822346 (2012).
- [5] Sowmiya C., Arun K. Thittai, *Proc. SPIE 10137*, 101371O (2017).

# Heteroepitaxy of Orientation-patterned GaP on GaAs Templates for Frequency Conversion Applications

A. Strömberg<sup>1</sup>, G. Omanakuttan<sup>1</sup>, H. Jang<sup>1</sup>, T. Mu, P. V. Natesan<sup>1</sup>, T. S. Tofa<sup>1</sup>, M. Bailly<sup>2</sup>, A. Grisard<sup>2</sup>, B. Gérard<sup>3</sup>, V. Pasiskevicius<sup>1</sup>, F. Laurell<sup>1</sup>, S. Lourdudoss<sup>1</sup>, Y. T. Sun<sup>1</sup>

1. Department of Applied Physics, Royal Institute of Technology-KTH, 106 91 Stockholm, Sweden

2. Thales Research & Technology, 1 av. A. Fresnel, 91767 Palaiseau, France

3. III-V Lab, 1 av. A. Fresnel, 91767 Palaiseau, France

GaP boasts excellent nonlinear properties making it suitable for terahertz (THz) and mid-IR generation by frequency down-conversion using quasi-phase-matching (QPM) schemes [1]. By growing OP-GaP on OP-GaAs templates by direct heteroepitaxy, the beneficial material properties of GaP can be combined with the high-quality substrates and mature processing techniques afforded by GaAs [2].

In this work, heteroepitaxy of OP-GaP on OP-GaAs templates prepared by a wafer bonding technique was performed using our low-pressure hydride vapor phase epitaxy (LPHVPE) reactor at 20 mbar and 710 °C. The effect on the growth by precursor gas flows was investigated to achieve good domain fidelity as well as high growth rate and crystalline quality. It was found that threading dislocations (TDs) caused by the 3.6% lattice mismatch between GaP and GaAs deteriorate the domain fidelity by enhancing the lateral growth rate of the (00 $\bar{1}$ ) domains. Increasing the GaCl flow reduced the TD density and resulted in OP-GaP with good domain fidelity and a high growth rate of 57  $\mu\text{m/h}$  (Fig. 1a). The crystalline quality of the OP-GaP growths were characterized by high resolution x-ray diffraction (HRXRD) reciprocal space mapping (RSM), in which the different domains can be resolved. A high crystalline quality of each domain is revealed by the low full width at half maximum (FWHM) value along the omega-direction in the RSM (Fig. 1b). THz transmission spectroscopy (TDS) was performed on a planar GaP reference sample grown on semi-insulating (SI) GaAs. The transmitted spectrum from the GaP layer was used to extract the conductivity in the THz range (0.2-0.9 THz). The conductivity was fitted to the Drude model (Fig. 1c) yielding a DC conductivity of 0.16 S/cm and a characteristic scattering time of 305 fs.

To summarize, OP-GaP was grown heteroepitaxially on wafer-bonded OP-GaAs template substrates by LPHVPE. High GaCl flows were used to achieve a high growth rate of 57  $\mu\text{m/h}$  as well as vertical domain boundaries by suppressing the formation of threading dislocations. A high crystalline quality was revealed by HRXRD RSM, and results from TDS on GaP grown on SI-GaAs were presented. The results presented here indicate that direct heteroepitaxy of OP-GaP on OP-GaAs templates are a promising approach for QPM-enabled THz and mid-IR frequency generation.

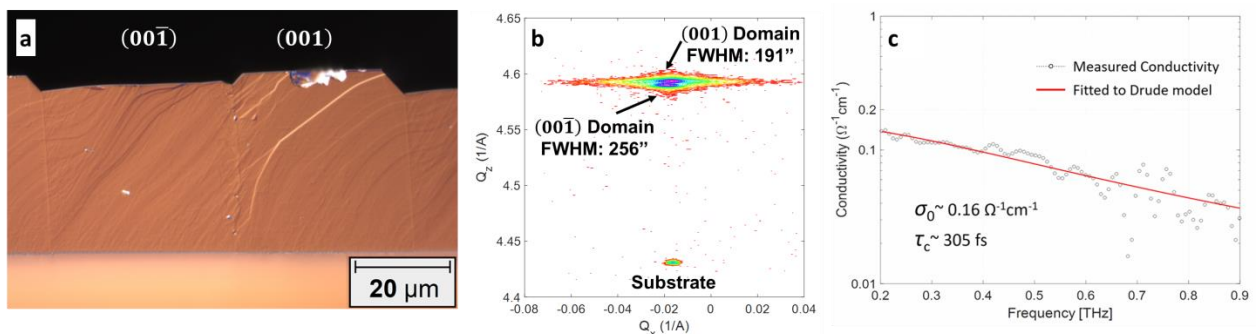


**Fig. 1:** (a) Microscopy image of OP-GaP on OP-GaAs template cross section grown with  $\text{PH}_3 = 50 \text{ sccm}$ , and  $\text{GaCl} = 25 \text{ sccm}$ . (b) HRXRD RSM of the OP-GaP growth on OP-GaAs template. (c) THz conductivity extracted from the THz transmission spectroscopy measurements and fitted to the Drude model.

## References:

- [1] P. G. Schunemann, K. T. Zawilski, L. A. Pomeranz, D. J. Creeden, P. A. Budni, *J. Opt. Soc. Am. B* **2016**, *33*, D36
- [2] V. L. Tassev, S. R. Vangala, *Crystals* **2019**, *9*, 39

# Micro- and Nanostructured TiO<sub>2</sub> Nanoparticles-Based Optical Coatings for LED and Solar Cell Applications

Dennis Visser<sup>1</sup>, Yohan Désières<sup>1,2</sup>, Ding Yuan Chen<sup>1</sup>, and Srinivasan Anand<sup>1</sup>

<sup>1</sup>*Department of Applied Physics, KTH Royal Institute of Technology,  
Electrum 229, SE-164 40 Kista, Sweden.*

<sup>2</sup>*CEA-LETI MINATEC, Grenoble, France.*

*Email: [dvisser@kth.se](mailto:dvisser@kth.se)*

Optical coatings are interesting for light manipulation functions to meet the demand for high energy efficient devices in the field of optoelectronics. For example, light emitting diodes (LEDs) show limited light extraction efficiency predominantly due to internal surface reflections. Surface microstructuring has been reported as an efficient way to enhance the light extraction efficiency of GaN-based LEDs. [1-3] For solar cells, the use of high refractive index materials (for example Si) results in high surface reflections (about 30-35% in the solar spectral region) and thus lower light absorption in the cell. By appropriate surface micro/nanopatterning, surface reflection can be reduced significantly by introducing light manipulation functions (anti-reflection, guiding and trapping).

In this work, a cost-effective and low-temperature/pressure table-top embossing method using nanoparticles-assemblies is developed and used to fabricate optical coatings consisting of assembled titanium dioxide (TiO<sub>2</sub>) nanoparticles (average size of ~50 nm). A polydimethylsiloxane (PDMS) mold was created using pre-patterned microcone and nanopillar array master molds. The fabricated PDMS molds were used as a stamp to directly print well-defined and large surface area micro- and nanostructure arrays on various substrates (e.g., Si, glass, GaAs, InP and GaN) relevant for solar cell and GaN-based LED devices. Electromagnetic modeling and simulations were performed to determine the optimal parameters for the desired optical functions – broadband anti-reflection for solar cells and light extraction enhancement in LEDs. In addition, the fabricated structures were optically characterized by spectrophotometry using total reflectivity and transmission measurements. Finally, we demonstrate direct embossing of structured optical coatings on c-Si, GaAs, and InP solar cells and vertical thin film (VTF) GaN-based LEDs. Performance improvements of these devices are analyzed both theoretically and experimentally, taking into account the optical properties of the structured coatings.

- [1] T. Fujii et al., *Appl. Phys. Lett.*, **84**(6), 855 (2004).
- [2] D.-H. Kim et al., *Appl. Phys. Lett.*, **87**(20), 203508 (2005).
- [3] K.-J. Byeon et al., *Appl. Surf. Sci.*, **346**, 354 (2015).

# Intra-Cavity Up-Conversion Photon Counting Mid-Infrared Range Determination

Max Widarsson<sup>1</sup>, Markus Henriksson<sup>2</sup>, Patrick Mutter<sup>1</sup>, Carlota Canalias<sup>1</sup>, Valdas Pasiskevicius<sup>1</sup>, and Fredrik Laurell<sup>1</sup>

<sup>1</sup>Royal Institute of Technology, Department of Applied Physics, 106 91 Stockholm, Sweden

<sup>2</sup>Swedish Defence Research Agency, 583 30 Linköping, Sweden

email: maxwida@kth.se

There are numerous interesting features in the mid-infrared (MIR) spectral region, such as molecular absorption fingerprints [1] and higher transmission through certain media due to the longer wavelength. Therefore, there is a desire to use MIR LIDARs to benefit from these features. One technique to achieve high resolution and sensitivity for LIDAR is to utilise photon counting [2]. Unfortunately, the available photon counters in the MIR are often limited in wavelength and are often based on either cooled detectors [3], or utilising InGaAs detectors [4]. Furthermore, these detectors have worse characteristics, such as temporal resolution, dark count rate and dead-time, than their equivalent in the visible and near infrared region, the Si-based detectors.

By utilising nonlinear interactions it is possible to up-convert MIR pulses through sum frequency generation into the visible spectral region [5,6] and therefore enables the possibility to reap both the benefits of the MIR and of the Si-based detectors. There are two main approaches for the sum frequency generation, either the nonlinear crystal can be inside the cavity of the pump beam [7], or the pump beam can operate in a single pass through the crystal [8]. The former requires a slightly more complex system but allows for significantly higher powers of the pump beam and therefore higher conversion efficiencies. By utilising quasi phase matched (QPM) structured crystals it is possible to select the detected wavelength as well as the acceptance bandwidth.

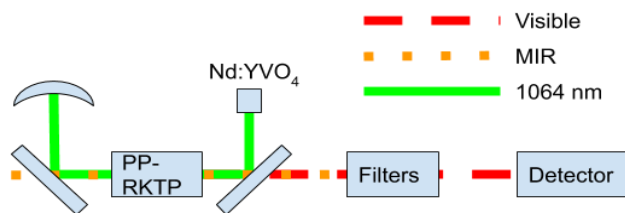


Fig. 1: A sketch of the detection cavity. The green line represents the oscillating 1,064 nm, the orange represents the MIR light and the red represents the up-converted visible light.

This work utilised a periodically poled rubidium doped  $\text{KTiOPO}_4$  (PPRKTP) crystal with a grating period of  $23.5 \mu\text{m}$  and a grating length of 9 mm. The crystal was inserted in a 1,064 nm Nd:YVO<sub>4</sub> cavity. This allowed for  $2.4 \mu\text{m}$  pulses to be converted to 737 nm. These pulses could then be detected in a Si- single photon avalanche photodiode. In Fig. 1 a sketch of the layout for the up-converted detection scheme can be seen. This

technique allows for excellent characteristics, essentially only limited by the visible detector and electronics. Therefore, good temporal and range resolution of LIDAR traces is obtainable.

## References

- [1] X. Yang, R. Lindberg, J. Larsson, J. Bood, M. Brydegaard, and F.k Laurell, *Opt. Express* **27**, 10304, 2019.
- [2] C. J. Grund and E. W. Eloranta *Optical Engineering*, **30** (1), 6, 1991.
- [3] R. E. Warburton et al, *Opt. Lett.* **32**, 2266-2268, 2007.
- [4] M. Henriksson, L. Allard, P. Jonsson, *Electro-Optical Remote Sensing XII*, Proceedings Volume **10796**, 1079606, 2018
- [5] L. Høgstedt, A.Fix, M. Wirth, C. Pedersen, and P. Tidemand-Lichtenberg. *Opt. Express*, **24**, 5152, 2016.
- [6] Haiyun. Xia et al, *Opt. Lett*, **40**, 1579, 2015.
- [7] J. S. Dam, P. Tidemand-Lichtenberg and C. Pedersen, *Nat. Photonics*. **6**, 788, 2012.
- [8] G. Temporão, S. Tanzilli, H. Zbinden, and N. Gisin, *Opt. Lett.* **31**, 1094, 2006.

# Mueller Matrix Spectroscopic Tomography of Inhomogeneous Anisotropic Media

Qulei Xu<sup>a,b</sup>, Yingjie Yu<sup>a</sup>, Sergiy Valyukh<sup>b\*</sup>

<sup>a</sup>*Department of Precision Mechanical Engineering, Shanghai University, Shanghai 200072, China*

<sup>b</sup>*Department of Physics, Chemistry and Biology Linköping University, SE-581 83 Linköping, Sweden*

*\*email:sergiy.valyukh@liu.se*

Inhomogeneous transparent materials, e.g. liquid crystals, due to their ability to affect the light polarization and direction of propagation find use in various optical and photonic applications. Liquid crystal displays and spatial light modulators are an excellent example. Performance of these applications are critically depend on parameters of the materials used, as well as on the character of inhomogeneity [1-3]. Therefore, accurate measurements methods for such media are of great importance. Similar tasks are required in photoelasticity where deformations and distribution of external forces are investigated by optical response measurements. The reported measuring methods are based on the fact that the spatial distribution of inhomogeneity is known [4, 5]. However, this is not always the case. Cancer, geological structures, arbitrary deformed transparent materials, some liquid crystals and many other media possess preliminary unknown spatial distribution of the optical axis. The situation for measurements became specially complicated when in additional to linear anisotropy a material has gyrotropy and dichroism.

In this presentation we report about our work on the Mueller matrix spectroscopic ellipsometric technique that in combination with traditional methods of optical tomography based on the principles of integrated geometry enables us to reconstruct 3-dimensional (3D) image of inner structure of a tested material. To do this, we get a set of 2-dimensional (2D) measured projections in a form of Mueller matrixes at different angles. The measured Mueller matrixes for each projection are decomposed and presented as integrated values of linear and circular birefringence and dichroism. By applying the inverse Radon transformation to the resulting set of data, we get information about spatial and spectral distributions of linear and circular birefringence and dichroism. This technique opens new attractive perspectives for characterization materials and their defects in science, medicine and industry.

## *Reference*

1. S. Valyukh, V. Chigrinov, H. S. Kwok, H. Arwin, *Opt. Expr.* 20, 15209-15221 (2012).
2. S. Valyukh, H. Arwin, J. Birch, K. Järrendahl, *Opt. Mater.*, 72, 334-340 (2017).
4. S. Valyukh, I. Valyukh, V. Chigrinov, H.S. Kwok, H. Arwin, *Appl. Phys. Let.* 97, 231120 (2010).
4. S. Valyukh, S. Sorokin, V. Chigrinov, *J. Displ.Tech.*, 11(12), 1042-1047 (2015).
5. S. Valyukh, I. Valyukh, H. Arwin, V. Chigrinov, 102, 063110 (2007).

SPONSORS



SPONSOR OF THE PS AND SOS STUDENT AWARD 2019

1<sup>ST</sup> PRIZE



2<sup>ND</sup> PRIZE



POSTER AWARD



MEDIA PARTNERS



SUPPORTED BY



EXHIBITORS

